

Electrochemical Investigation on Electroless Fe–B Deposition

Gui-Fang Huang^{1*}, Wei-Qing Huang¹, Ling-Ling Wang¹, Yi-Cun Zhu¹, Jian-Hui Zhang², Qiao-Ling Wang²

¹Department of Applied Physics, Hunan University, Changsha 410082, PR China

²Changsha Environmental protection College, Changsha 410004, PR China

*E-mail: gfhuang@hnu.cn or huanggfhao@yahoo.com

Received: 29 August 2006 / Accepted: 26 September 2006 / Published: 1 November 2006

In this paper we investigate the effects of plating parameters such as the coupled aluminum, bath composition and bath temperature on Fe-B electroless deposition by electrochemical method. The results show that coupled aluminum induces the Fe-B electroless deposition by shifting the potential negatively and decreasing the polarization resistance of anodic and/or cathodic reaction. The variations of the bath composition and temperature shift the mixed potential and change deposition rate of Fe-B electroless deposition. Due to the interactions between the two half reactions on the catalytic surface, the plating rate determined by electrochemical measurement in the complete bath is higher than that determined from the simulation half-reaction cells.

Keywords: Electroless deposition, Electrochemical, Fe-B

1. INTRODUCTION

It is widely accepted that electroless plating proceeds along the electrochemical mechanism as a simultaneous reaction of cathodic metal deposition and anodic oxidation of a reductant took place on the same catalytic surface. Based on the Wagner-Traud mixed potential theory of corrosion process, the deposition rate of an electroless process can be calculated by polarization measurement in the

complete bath, $i_{d1} = \frac{K}{R_p}$ (1)

in which $K(= \frac{b_a b_c}{2.303(b_a + b_c)})$, here, b_a and b_c are the anodic and cathodic Tafel slopes) is the polarization constant, R_p is the polarization resistance.

The two half-reactions in electroless deposition may be represented in general form as: cathodic reduction reaction $ML_m^{n+} + ne = M + mL$, and anodic oxidation reaction $Red(aq) = Ox(aq) + xe$. The partial cathodic or partial anodic polarization that would occur in the complete electroless can be simulated by polarization experiments in the baths absence of either metallic ions or reductants. Many researches on independent partial reactions were carried out in the electroless Cu, Ni-P, Co-P and their alloys baths [1-5]. Good agreement between the measurement of instantaneous deposition rate calculated from the partial reaction data and the average deposition rate determined gravimetrically in the case of Ni-P, Co-P and Co-W-P was obtained[4-6].

Fe-B films have good magnetic properties and are very useful for various applications [7-9]. Various methods such as sputtering, pulsed laser deposition, and electron-beam evaporation are effective to obtain Fe-B films[9-11]. However, these methods become inconvenient to deposit films on large area surface with different shapes. Electroless deposition is a chemical method to obtain homogeneous films on various substrate and is applied in wide industrial fields[12-21]. Electroless Fe-B films were first prepared by Hu and Zhang[22]. Their work and other groups' work obtained successfully Fe-B electroless deposits from a chemical bath by connecting the substrate with an aluminum foil during deposition and investigated the composition, structure, magnetism, mechanical and anti-corrosion behavior of deposits[22-26]. But few reports on the inducing effect of connected aluminum and the half reactions involved in Fe-B electroless deposition are available.

This work is dedicated to the investigation of the electroless Fe-B deposition systems. The inducing effect of coupled aluminum on Fe-B deposition was studied and effects of certain plating parameters on the plating rate of electroless Fe-B deposition were studied. The polarization measurement in the complete bath and the partial cathodic or partial anodic polarization measurement in the baths in the absence of either metallic ions or reductants were carried and the mixed potential and deposition current determined by the two measurements were compared.

2. EXPERIMENTAL PART

The brass electrode ($\phi = 19mm$) embedded in an epoxy resin was used as substrate. The bath compositions are given in Table 1. The substrate and aluminum foil were orderly polished with #600, #1200, and #2000 emery paper, and then rinsed by de-ionized water, diluted HCl, de-ionized water, acetone, de-ionized water, alcohol in sequence prior to deposition. During deposition, the substrate was connected with aluminum foil through a copper wire.

Table 1. The bath compositions of electroless Fe-B depositions

Reagents	Concentration (g/L)
KNaC ₄ H ₄ O ₆ ·4H ₂ O	75
FeSO ₄ ·7H ₂ O	10~30(20) ^a
KBH ₄	1.7~4.7(2.7)
NaOH	20~36(28)
C ₁₂ H ₁₂ O ₁₁	2

^a In brackets for constant value.

The electrochemical measurement was carried out in a three-compartment cell with the electrochemical analyzer CHI-660B. A platinum foil with size $20 \times 40 \text{ mm}^2$ was used as an auxiliary electrode and a saturated calomel electrode was used as reference electrode. The working electrode was the brass electrode connected with aluminum foil. The potentiostatic polarization measurement in the complete bath and the partial cathodic or partial anodic polarization investigation of the electrolytes in the absence of either the KBH_4 reducer (oxidation solution) or the FeSO_4 (reducing solution) was carried out.

3. RESULTS AND DISCUSSION

3.1 Electrochemical investigation on the inducing effect of coupled aluminum

Experiments found that there was no deposit on brass substrate unless the brass coupled with aluminum during deposition. To reveal the effect of the coupled aluminum on Fe-B deposition, the partial anodic and cathodic polarization curves were measured with or without the coupled aluminum foil. It is well known that the electroless deposition is classified as autocatalytic redox reactions with the metal as a final product in which both the cathodic reduction of the metal and the anodic oxidation of the reducing agent take place on the same catalytic surface. The difference between the redox potential of the reducing agent and that of the metal, ΔE , is the force to drive deposition and related to the reaction rate. When the potential difference ΔE is lower than zero, the deposition is difficult to take place. The I-E curves of brass in oxidation solution or reducing solution in Fig.1 (a) show that there is no intersection between the two curves, and the potential of brass electrode in reducing solution and oxidation solution were about -0.82 V and -0.85 V vs.SCE, respectively. Thus, the value of potential difference ΔE is negative and there is no force to drive deposition. In comparison, the potentials of brass connected with aluminum foil in reducing and oxidation solutions were about -1.38 V and -1.32 V vs.SCE, respectively, as displayed in Fig.1(b).

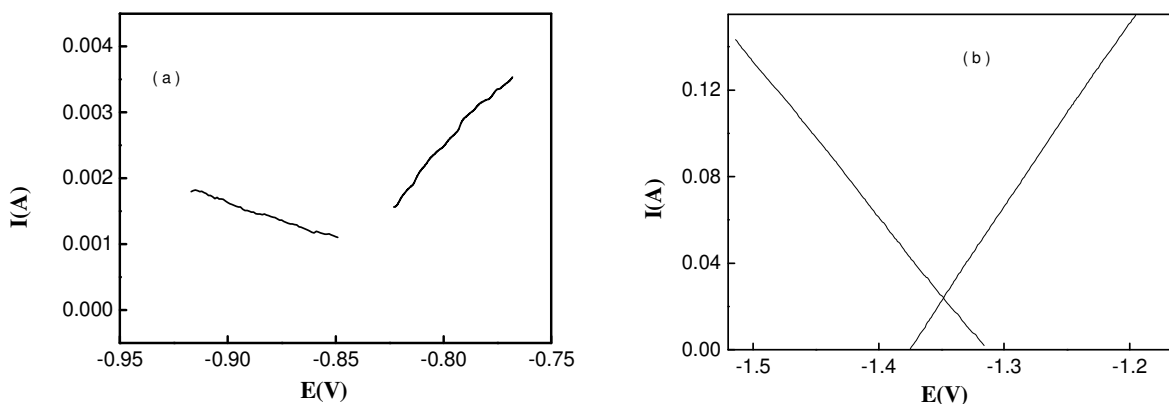


Figure 1. Partial cathodic I-E curve for reduction of Fe^{2+} ions and anodic polarization curve for oxidation of BH_4^- : (a) brass electrode, (b) brass electrode coupled with aluminum

The difference between the potential of the reducing agent and that of the metal, 0.06 V, is the electromotive force to drive deposition. The cathodic and anodic curves intersect at one point where the potential and the current is -1.35 V and 0.023 A, respectively. According to the mixed potential theory, the intersection of these two polarization curves represents mixed potential and deposition rate i_{d2} , i.e., the deposition reaction was carried out with a current of 0.023 A. The resistance for cathodic and anodic reaction (R_{pc} and R_{pa}) derived from the polarization curves are 1.39 and 1.17Ω , respectively, which are much less than those (106.6 and 2.73Ω , obtained from the polarization curves in Fig.1(a)) without coupled aluminum. Therefore, it can be concluded that the coupled aluminum keeps the substrate surface active and induces the Fe-B deposition by shifting the potential negatively and decreasing the anodic and/or cathodic reaction resistance.

3.2 Electrochemical investigation on the effects of plating parameters

The data presented in this section were obtained from partial polarization measurements carried out in the absence of either FeSO_4 (partial anodic curve) or KBH_4 (partial cathodic curve).

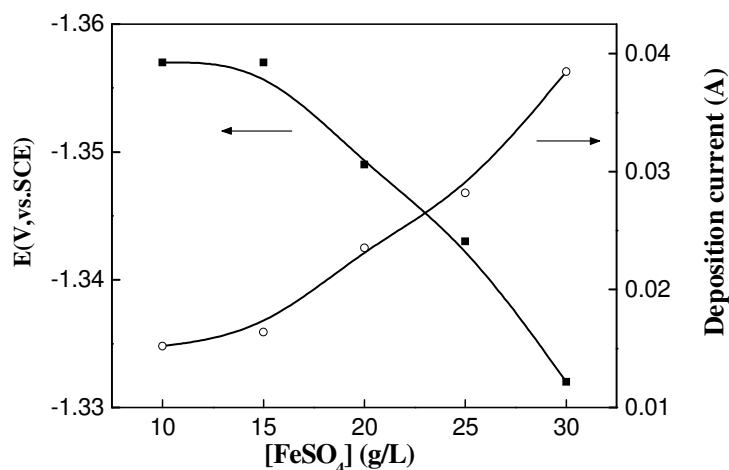


Figure 2. The dependence of the mixed potential and deposition rate on FeSO_4 concentration derived from partial polarization curves

The effect of FeSO_4 concentration on the mixed potential and deposition current is shown in Fig.2. It can be seen that the effect of concentration of the metal salt on the mixed potential and deposition current density is pronounced. The mixed potential shifts positively and the deposition current increases with increasing FeSO_4 concentration. The deposition current increase by more than twice when the FeSO_4 concentration varies from 10 to 30 g/L.

KBH_4 acts as reductant in the bath and supplies the element boron for the deposits. Fig.3 displays the effect of KBH_4 concentration on the mixed potential and deposition current. It can be seen that the mixed potential shifts positively slightly while the current increases first and decrease after a maximum with increasing KBH_4 concentration. It is well known that electroless deposition process is an autocatalytic process with the metal as a final product, based on the chemical reduction of the metal

cations through reductants in the bath. It is reasonable that the deposition current increases with the reductant concentration increase. The current decrease with the increase of KBH_4 concentration may be attributed to the decomposition of KBH_4 .

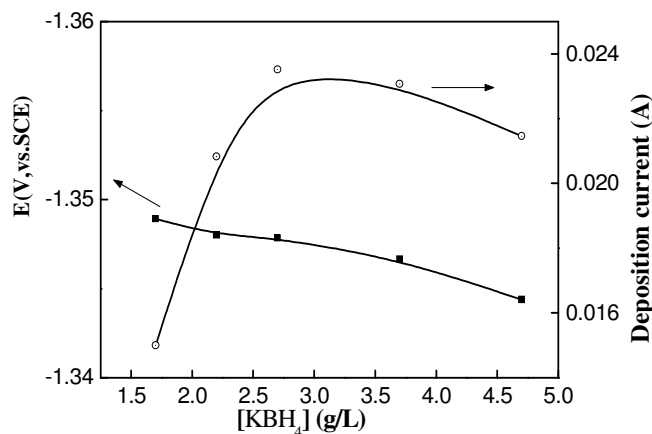


Figure 3. Dependence of the mixed potential and deposition rate on the $[\text{KBH}_4]$ derived from partial polarization curves

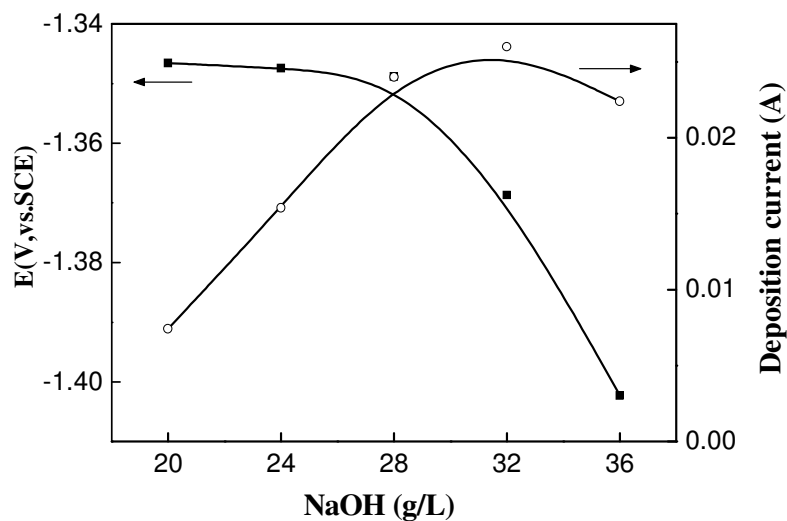


Figure 4. Dependence of the mixed potential and deposition rate on the pH

The pH has significant influence on the deposition current and mixed potential of the process. In this work, the pH of the solution was adjusted using NaOH. The dependence of the mixed potential and deposition current on the NaOH concentration, as derived from the polarization curves, is presented in Fig.4. It can be seen that the mixed potential shifts cathodically and the deposition current density increases with the NaOH concentration increasing. The mixed potential shifts by approximately 60 mV and the deposition current changes by more than a factor of 3 when the NaOH

concentration varies from 20 to 26 g/L. This trend was similar to that observed for electroless Fe-P, Co-W-P and Co-P deposition[6,27].

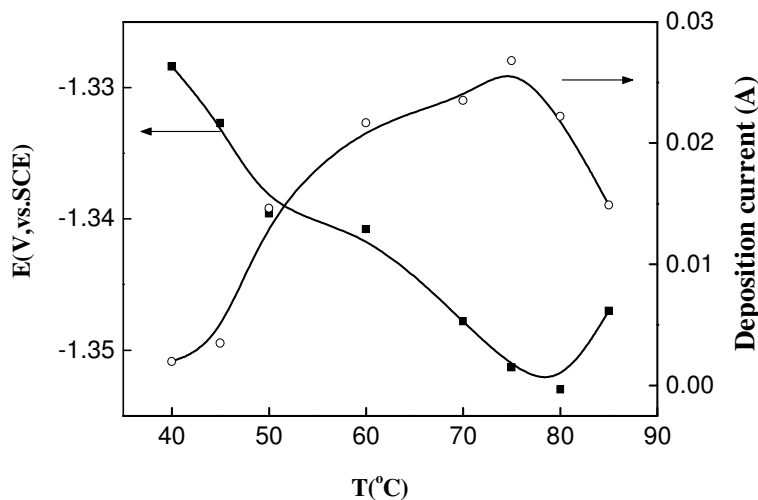


Figure 5. Dependence of the mixed potential and deposition rate on the bath temperature

Fig.5 depicts the dependence of the mixed potential and deposition current on the temperature, as derived from electrochemical measurements. At low temperatures, the process is very slow and may not start below 50°C. When the temperature varies from 45 to 75°C, the mixed potential shifts negatively and the current increases with increasing temperature, while the mixed potential shifts positively and the current decreases with the further increase of temperature. The temperature of electroless bath is one of the important factors affecting the deposition rate. It is true that the deposition rate increases with the temperature increase for almost all the systems. However, as the operating temperature is beyond a certain value, the bath tends to become unstable[28].

3.3 The comparison of mixed potential and deposition current determined from the two polarization measurements

To study of the interactions between the two half-reactions i.e., cathodic and anodic reaction, in electroless plating, the potential dependences of both the cathodic and anodic half reaction current were measured both in the complete plating bath and in the modified solutions where either the cathodic or the anodic half reaction can be investigated in isolation.

Fig.6 illustrates the polarization curves, which were obtained by scanning the potential at a rate of 1 mV s^{-1} in the range $\pm 150 \text{ mV}$ of the open circuit potential E_{mix} in the electroless Fe-B complete bath with different FeSO_4 concentration. The anodic b_a and cathodic b_c Tafel slopes were evaluated from these polarization curves, and the polarization resistance was determined from the linear polarization experiments by scanning the potential $\pm 15 \text{ mV}$ about the open circuit potential at the same rate. The deposition current was calculated using equation (1). The mixed potential and deposition current

determined from these curves are presented in Fig.7. It can be seen that the dependence of the mixed potential and deposition current on FeSO_4 concentration shows similar tendency to that derived from partial polarization curves as shown in Fig.2, i.e., the mixed potential shifts positively and the deposition current increases with increasing FeSO_4 concentration.

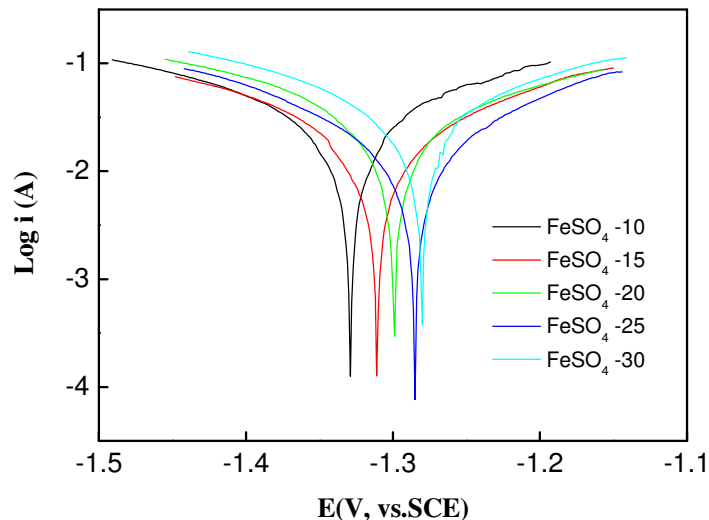


Figure 6. *I-E* curves in the electroless Fe-B complete bath

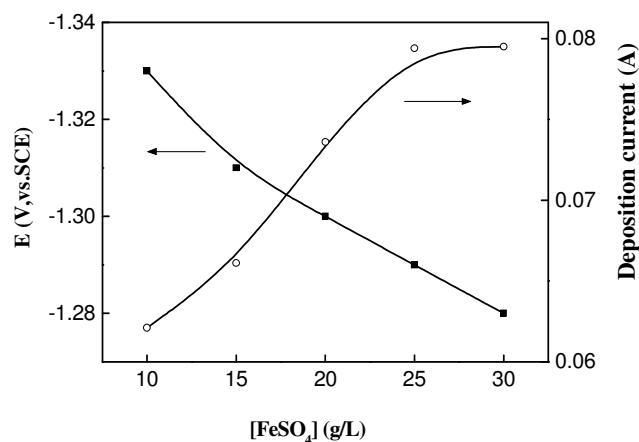


Figure 7. The dependence of the mixed potential and deposition current on FeSO_4 concentration derived from polarization in the complete bath

However, the mixed potential determined from the polarization in the complete bath is a little positive to that derived from the partial polarization curves, and deposition current from the polarization in the complete bath is large than that from the partial polarization curves. The possible

reason for the magnitude difference between the deposition current derived from the polarization curves in the complete bath and that in the simulation half-reaction cells is that the reduction of iron ions and hypophosphite is accelerated to some extent due to the interaction between the two half reactions on the catalytic surface.

4. CONCLUSIONS

The inducing effect of coupled aluminum on electroless Fe-B deposition was investigated by electrochemical measurement. The coupled aluminum induces the Fe-B deposition by shifting the potential negatively and reducing the reaction resistance. The change of the parameters such as bath composition and bath temperature will result in the variation of mixed potential and deposition current. With the change of plating parameters, the deposition rate derived from polarization curves in the complete baths show similar tendency to that expected from a combination of the appropriate simulation anodic and cathodic polarization curves. The magnitude difference between the deposition current derived from the polarization curves in the complete bath and that in the simulation half-reaction cells implies that the anodic and cathodic reactions are interdependent when they occur simultaneously.

ACKNOWLEDGMENTS

This work was supported by Hunan Provincial Natural Science Foundation of China (Grant No. 05JJ30089).

References

1. A.H.Gafin, S.W.Orchard, *Journal of Applied Electrochemistry*, 22(1992) 830
2. B. Veeraraghavan, H. Kim and B. Popov, *Electrochimica Acta*, 49(2004)3143
3. M. Paunovic, *Plating*, 55 (1968)1161
4. I. Ohno, S. Haruyama, *Surface Technology*, 13 (1981)1
5. I. Ohno, O. Wakabayashi, S. Haruyama, *Journal of the Electrochemical.Society*, 132 (1973)739
6. N. Petrov, Y. Sverdlov, and Y. Shacham-Diamand, *Journal of the Electrochemical.Society*, 149(2002)C187
7. S. Oswald, S. Fahler and S. Baunack, *Applied Surface Science*, 252 (2005)218
8. M. Venkatesan, J. Buschbeck, Fernando M. F. Rhen and J. M. D. Coey, *Journal of Magnetism and Magnetic Materials*, 272-276(2004)E881
9. H. Fukunaga, M. Nakano, Y. Matsuura, H. Takehara and F. Yamashita , *Journal of Alloys and Compounds*, 408-412(2006)1355
10. M. Valetas, M. Verite, A. Bessaudou, F. Cosset and J.C. Vareille, *Computational Materials Science*, 33(2005)163
11. V. V. Uglov, J. A. Fedotova, J. Stanek, *Surface and Coatings Technology*, 128-129(2000)351
12. Yosi Shacham-Diamand, A. Inberg, Y. Sverdlov, V. Bogush, N. Croitoru, H. Moscovich and A. Freeman, *Electrochimica Acta*, 48 (2003)2987
13. Y. Shacham-Diamand, A. Zylberman, N. Petrov and Y. Sverdlov, *Microelectronic Engineering*, 64 (2002)315
14. H. Einati, V. Bogush and Y. Sverdlov, Yuri Rosenberg and Yosi Shacham-Diamand, *Microelectronic Engineering*, 82 (2005)623
15. J. F. Rohan, G.. O’Riordan and J. Boardman, *Applied Surface Science*, 185(2002)289

16. P. Peeters, G. v. d. Hoorn, T. Daenen, A. Kurowski and G. Staikov, *Electrochimica Acta*, 47(2001)161
17. A. Inberg, Y. Shacham-Diamand, E. Rabinovich, G. Golan and N. Croitoru, *Thin Solid Films*, 389(2001)213
18. A. Kohn, M. Eizenberg, Y. Shacham-Diamand, *Materials Science and Engineering A*, 302(2001) 18
19. Y. Shacham-Diamand, V. Dubin and M. Angyal, *Thin Solid Films*, 262(1995)93
20. J. LaPlante, *Metal Finishing*, 103(2005)18
21. T. Osaka, N. Takano and T. Yokoshima, *Surface and Coatings Technology*, 169-170(2003)1
22. W.Y. Hu, B.W. Zhang, *Physica B* 175 (1991) 396.
23. B.W. Zhang, W.Y. Hu, D.Q. Zhu, *Physica B* 183 (1993) 205.
24. W.Y. Hu, and B.W. Zhang, *Trans.Inst.Metal Finish*, 71(1993)30
25. N. FuJita, A. Tanaka, E. Makino, Patrick T. Squire, Pang Boey Lim, Mitsuteru Inoue and Toshitaka Fujii, *Applied Surface Science*, 113-114(1997)61
26. L.L Wang, L.H. Zhao, B.W. Zhang, Wangyu Hu, Xiaolin Shu, Xia Sheng and Zhiyuan Fang, *Journal of Alloys and Compounds*, 287(1999)234
27. G.F Huang, W.Q Huang, L.L. Wang, Y. Meng, Z. Xie and B.S. Zou, *Electrochimica Acta*, 51(2006)4471
28. R.C. Agarwala, V. Agarwala, *Sadhana*, Parts 3-4, 28(2003)475